STARTING FLOWS PAST SPHERES AND ELLIPTIC CYLINDERS

HONJI, Hiroyuki
Research Institute for Applied Mechanics, Kyushu University : Lecturer

https://doi.org/10.5109/7172228

出版情報：Reports of Research Institute for Applied Mechanics. 19 (65), pp.271-281, 1972. 九州大学応用力学研究所
バージョン：
権利関係：

Reports of Research Institute for Applied Mechanics
Vol. XIX, No. 65, 1972

STARTING FLOWS PAST SPHERES AND ELLIPTIC CYLINDERS*

By Hiroyuki HONJI**

The unsteady starting flow past either a sphere or an elliptic cylinder was investigated using flow visualization techniques. The Reynolds number ranges examined were from 62 to 1500 for the sphere experiment, and from 50 to 600 for the elliptic-cylinder experiment. The following results were found. (1) Irrotational flow pattern is always established around the test bodies at the beginning of motion. (2) For spheres, as time advances, a symmetric ring vortex grows behind the body, and the time dependence of the development of its flow direction length is approximately logarithmic. (3) The embryo of a localized secondary vortex appears around a Reynolds number of 1500 between the rear of the sphere and the main vortex. (4) For elliptic cylinders, the initial formation of a wake bubble behind the rear side of the cylinder is affected by the prescribed angle of attack considerably. (5) The visualized flow pattern variation for a 45° flat plate agrees well with the calculated result of Lugt and Haussling. (6) For an elliptic cylinder placed with its major axis normal to the uniform flow, the vortex length development with time seems to have a slight anomaly at about $U_0t/2c = 4.5$, where U_0 is the undisturbed flow velocity, t is the time elapsed since starting, and c is the distance between the foci.

1. Introduction

Recent development of high speed computers has made it possible to calculate time-dependent evolution of streamlines of unsteady viscous flow past various types of obstacles. At present, however, it seems to be necessary as yet that calculated results are verified minutely by the relevant experiment. Experimental studies of the starting flow past a circular cylinder and that past a 90° flat plate were already made some years ago by Taneda and the present author[1,2,3], and the general features of starting flow were clarified there.

The present work is concerned with the experimental study of time-dependent starting flows past two kinds of bodies having fundamental geometry: three dimensional flow past a sphere and two dimensional flow past an elliptic

* This work was read at the Annual Meeting of the Physical Society of Japan held in Sapporo (October 1, 1971).
** Lecturer, Research Institute for Applied Mechanics, Kyushu University.

cylinder at various angles of attack. For the present, experimental data on both of these flows seem to be very scanty.

The study of unsteady flow past a sphere was initiated by Boltze[4], who worked out the problem of the boundary layer on the sphere. From his time, many similar investigations have been made on the problem. Recently Rimon and Cheng[5] studied the impulsive starting flow past a sphere and predicted the temporal development of streamlines at various Reynolds numbers theoretically. They also obtained the Reynolds number dependence of the drag coefficient. Comparison in the vortex length will be made later.

The flow past an elliptic cylinder is of particular interest because a circular cylinder and a flat plate correspond to the small and the large limits of the eccentricity of its cross section respectively. Recent studies of the flow past an elliptic cylinder are those by Wang[6] and Lugt & Haussling[7]. Wang[6] was concerned only with the early stages of the boundary layer growth on the cylinder, while Lugt and Haussling[7] studied the flow around a flat plate at various angles of attack including the later stages of streamline evolution. Their plate is, as a matter of fact, an elliptic cylinder with the cross section of very high eccentricity. Periodic flows past inclined flat plates at later stages are of related interest; these stages were formerly studied by Fage and Johansen experimentally in greater detail. Flow past an elliptic cylinder at zero angle of attack was also studied by Richards[9]. The present work is concerned only with the initial laminar stages of unsteady flow past an impulsively started elliptic cylinder. Many photographs of flow patterns are included at the end of the paper because this work has been made with particular interest in the time-dependent development of unsteady flow streamlines.

2. Experimental Methods

Experiments were carried out using two water tanks separately; a 40 cm × 38 cm × 2 m tank for studying flow past a sphere, and a 50 cm × 50 cm × 6 m tank for flow past an elliptic cylinder ; see for details refs. 1 and 2. In the 2 m water tank impulsive starting was achieved by coupling a carriage of the test sphere with a rotating lead screw, and the carriage speed could be varied between 0.050 cm/s and 5.0 cm/s. Since for the elliptic cylinder experiment it seemed necessary to eliminate the effects of walls and the end of the test cylinder, the larger tank described above was employed. In this 6 m tank, a towing carriage could be moved to start with initial uniform accelerations between about 0.005 cm/s^2 and 9 cm/s^2. As it was impossible, however, to make impulsive starting using this apparatus, alternative nearly impulsive motions were examined; a test cylinder was made to start with the given large acceleration of 6.30 cm/s^2, and after attaining of the prescribed speed it was maintained constant. Such a motion would be considered as a good approximation to impulsive one, when the time interval of initial acceleration is very short compared with the time interval between the time of starting and the time of observation ; see Fig. 1.

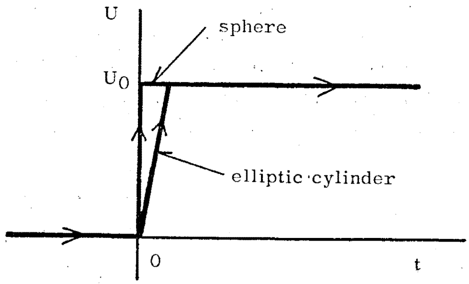

Fig. 1 Motion of test bodies

Fluid motion was visualized by means of the almiunm dust method; the electrolysis method was also employed only partly. A thin horizontal layer of water was illuminated by a 1 kw light source through a slit. In the sphere experiment the illuminated layer was adjusted so as to include the meridian section of the test sphere. After starting of test bodies, instantaneous flow patterns were photographed consecutively until the laminar flow regime collapsed using a camera driven by a motor automatically. Times elapsed since starting of the motion were determined by reading oscillograms recorded by means of an electromagnetic oscillograph. The middle of the time of exposure is always adopted as the 'time of observation'.

Specially made steel balls with diameters 3.00 cm and 5.08 cm were used as test spheres; the 3.00 cm sphere was suspended in water using a 0.1 mm piano wire, and for the 5.08 cm sphere a copper support rod of 0.2 cm diameter was used. Elliptic-cylinder models were three well-polished wooden cylinders, the length of which was 30.0 cm. One flat plate (3.00 cm in width and 30.0 cm in length) made of brass was also included.

3. Flow Patterns Around Spheres

The typical time-wise variation of streamlines at a low Reynolds number is presented in Photo 1. The Reynolds number is here defined as $R=U_0d/\nu$, and the dimensionless time as $\tau=U_0t/d$, where U_0 is the sphere speed with respect to the undisturbed water, d the sphere diameter, and t the elapsed time since starting. An irrotational flow is established at the beginning of motion, as will be seen from Photo 1-(a). As time increases, the boundary layer formation and separation begin on the body, and the symmetric ring vortex grows behind it. Although the flow is three-dimensional in this case, the general qualitative feature of flow pattern variation is not different from that for a circular cylinder.

Another example of flow pattern variation at a relatively high value of R is shown in Photo 2. From these photographs it will be seen that an embryo of small secondary vortex is formed upstream of the main vortex. The similar phenomenon occurs always in the unsteady flow past a circular cylinder when $R \geqslant 500$, as already reported in ref. 1. This secondary vortex collapses at the same time when the main vortex collapses.

The flow-direction vortex length was measured from many photographs of the instantaneous flow patterns. The vortex length s is measured from the rear end of a sphere. Fig. 2 shows s/d plotted against the dimensionless

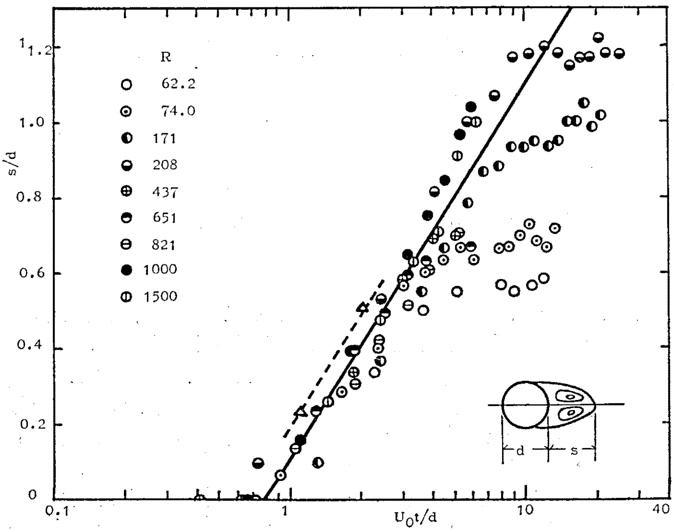

Fig. 2 Vortex length plotted against the dimensionless time: △, Rimon and Chen[4] (R=300).

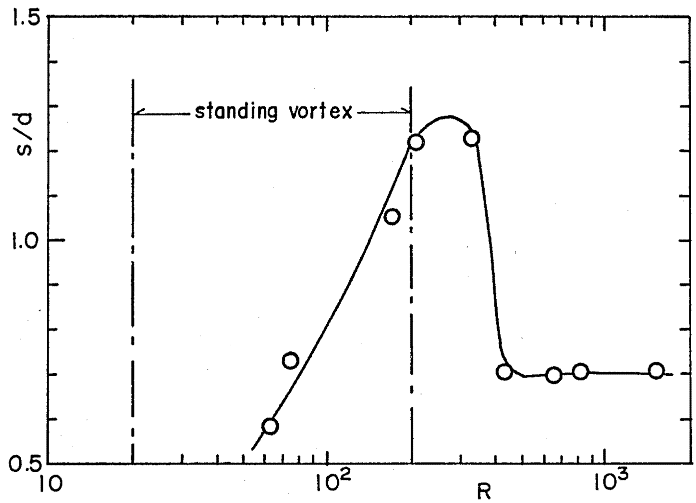

Fig. 3 Reynolds number dependence of the largest vortex length.

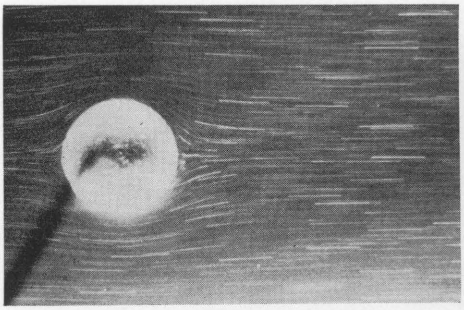

(a) $t = 1.50$ s, $U_0t/d = 0.395$

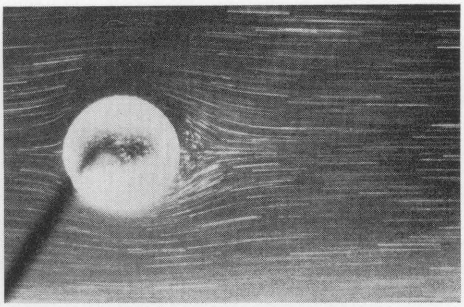

(b) $t = 4.88$ s, $U_0t/d = 1.29$

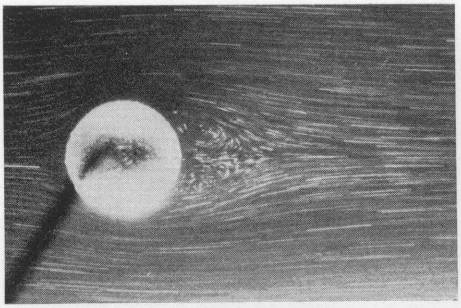

(c) $t = 13.6$ s, $U_0t/d = 3.58$

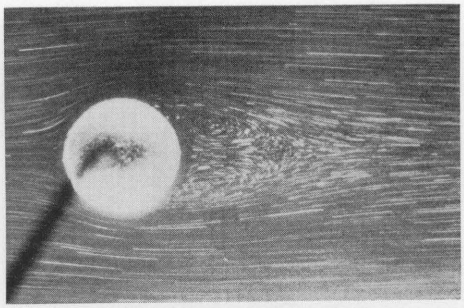

(d) $t = 37.5$ s, $U_0t/d = 9.87$

Photo 1 Time dependent variation of flow pattern around an impulsively started sphere at $R=172$; $U_0=0.790$ cm/s, $d=3.00$ cm, t_e (time of exposure) $=3.0$s.

(*Facing* p. 274)

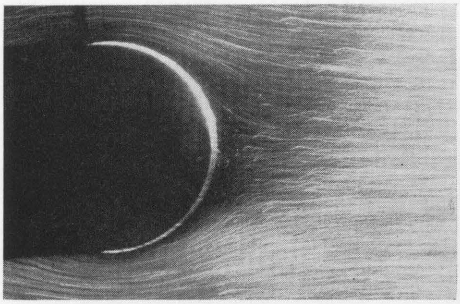

(a) $t = 0.72$ s, $U_0t/d = 0.401$

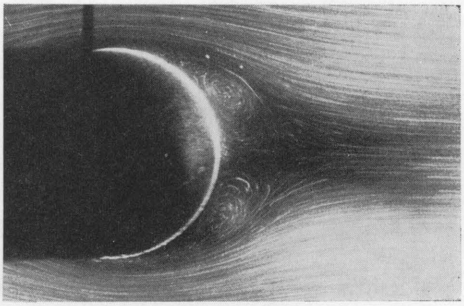

(b) $t = 2.56$ s, $U_0t/d = 1.43$

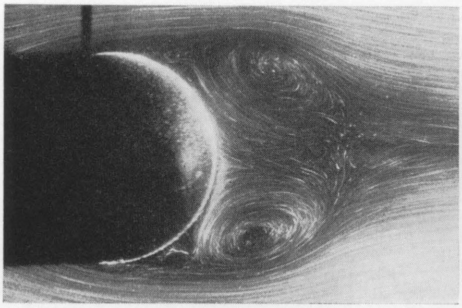

(c) $t = 6.04$ s, $U_0t/d = 3.36$

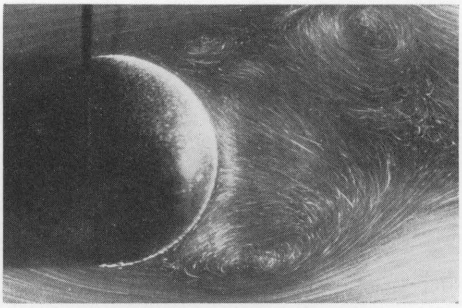

(d) $t = 11.0$ s, $U_0t/d = 6.13$

Photo 2 Same as Photo 1, at $R = 1500$; $U_0 = 2.83$ cm/s, $d = 5.08$ cm.

time U_0t/d at various values of R. s/d is nearly proportional to the logarithm of τ as in the case of steady flow past a sphere ; see ref. 10. The theoretical values at $R=300$ of Rimon and Cheng[4] are reproduced in the figure. The experimental data lie somewhat below the predicted curve. In the study of flow around circular cylinders, the similar features were reported by Hamielec and Raal[11], who pointed out that the deviation may arise from the presence of walls in the experimental measurement. It is, however, uncertain whether the same is responsible for the discrepancy described above. As will be seen from Fig. 3, the vortex having the largest flow-direction length was found to be observed around $R=300$; the standing vortex is known to exist for the approximate range $20<R<200$. The value of U_0t/d at which the largest symmetric vortex collapses is shown in Fig. 4, which shows that such a critical time decreases with R. The flow-direction vortex length and the position of vortex centers (when viewed two-dimensionally) at $R=1000$ are presented in Fig. 5.

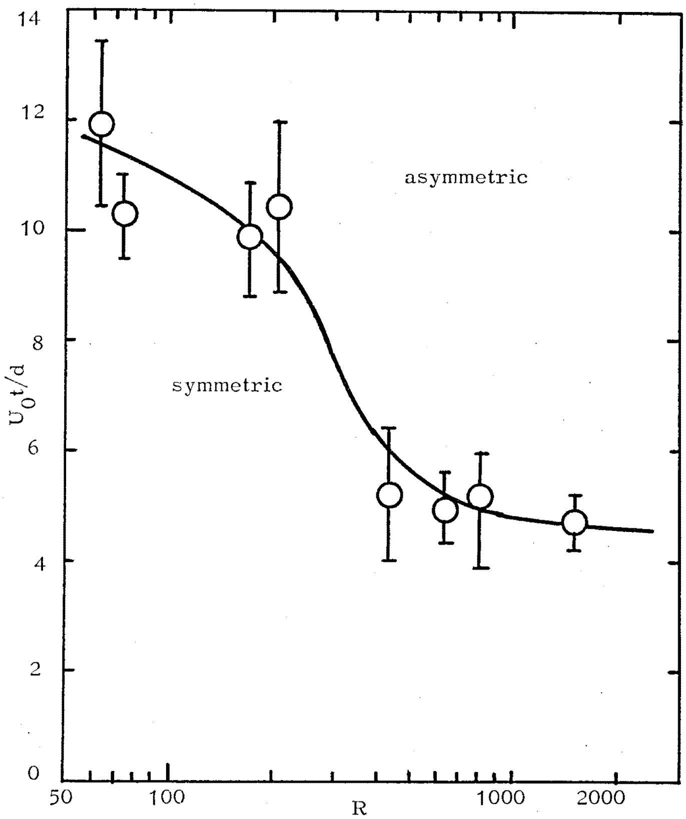

Fig. 4 Reynolds number dependence of dimensionless time at which symmetry of vortex is lost.

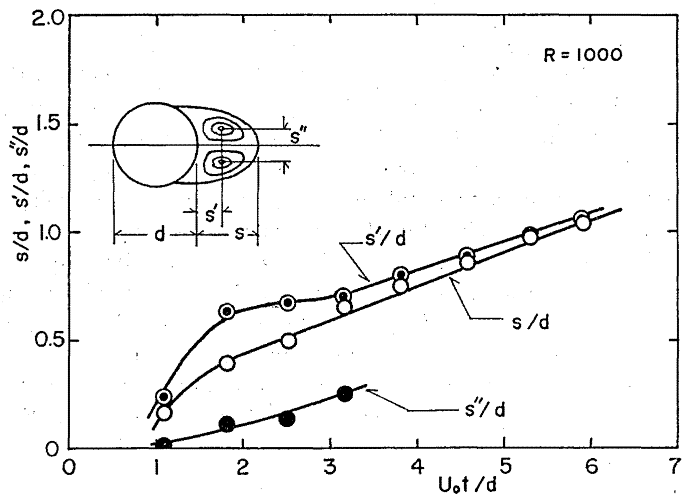

Fig. 5 Vortex length and position of vortex centers at $R=1000$.

4. Flow Patterns Around Elliptic Cylinders

As already mentioned in 2, three cylinders were used as the test elliptic cylinders, whose values of b/a are 0.558 ($e=0.809$), 0.500 (0.866), and 0.333 (0.943) respectively, a being half the length of the major axis, b half the length of the minor axis, and e the eccentricity, i. e. $e=\sqrt{1-(b/a)^2}$ the values of which are given in parentheses (see Fig. 6). As the limiting case of $e\approx 1$, the flow past a flat plate having some angle of attack was also examined. The Reynolds number and the dimensionless time are here defined based on $2c=2\sqrt{a^2-b^2}$, the distance between foci.

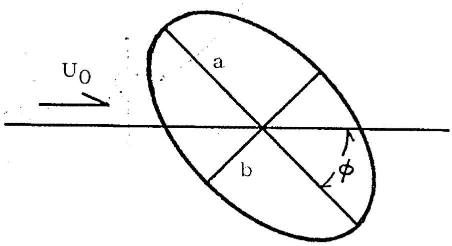

Fig. 6 Elliptic cylinder.

Photo 3 shows a series of pictures of how the flow pattern changes with time. At the beginning of motion the irrotational flow is established around the cylinder. Such a velocity field may be determined easily from the well-known form of the complex potential; see for example §6. 10 of ref. 12. As time advances, one wake bubble appears behind the cylinder, and then it grows until the periodic vortex shedding begins. This will be more clearly seen from Photo 4, which shows the time-wise motion of vortex sheets visualized by means of the electrolysis method; for this method see ref. 2. The movement of dye element accumulated on the cylinder surface is first dominated by the potential flow. At next instant the layer of intense vorticity separates from both leading and trailing edges. At moderate angles of attack the vortex separated from the leading edge covers the downstream region of the cylinder. It should be noted here that the dye element follows the actual fluid motion with some time-lag, and does not always show the region of the most intense vorticity.

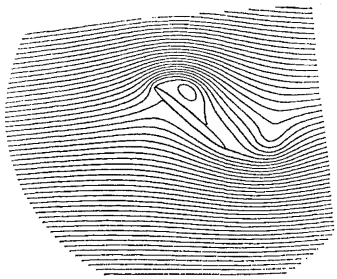

Fig. 7 Computed streamlines at $R=200$ and $U_0t/2c=0.74$. Reproduced with permission from Lugt and Haussling[7] (1972); compare with Photo 5 (b).

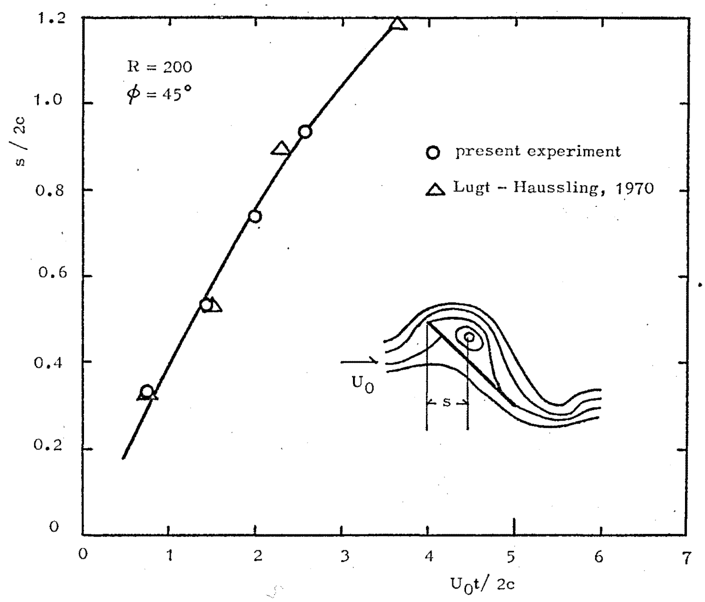

Fig. 8 Comparison of position of vortex center with theoretical prediction by Lugt and Haussling[7].

As a limiting case of large eccentricity, the starting flow past a flat plate at some angles of attack was investigated. Photo 5 shows the time-dependent development of the streamlines. It will be seen from this figure that the feature of the flow pattern evolution is essentially similar to that for elliptic cylinders with e of nearly unity. Lugt and Haussling[7] calculated the streamline development for a 45° elliptic cylinder with very large eccentricity at various R. Fig. 7 shows an example of streamlines at R=200 obtained by them. The general agreement with the present work seems to be good. For example, Fig. 8 shows the time-wise evolution of the distance between a

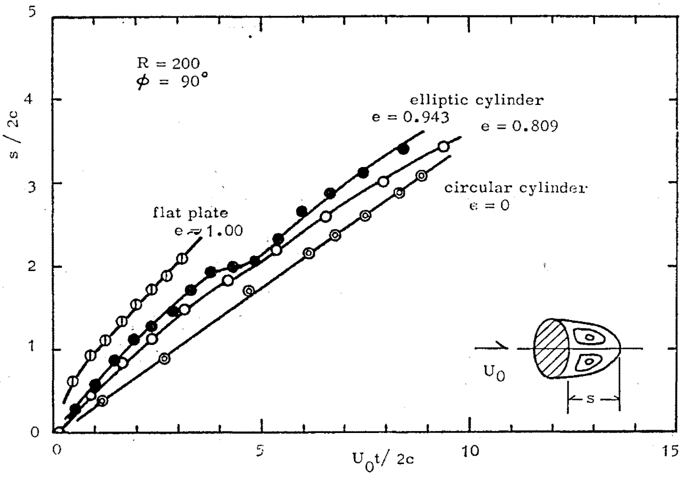

Fig. 9 $S/2c-U_0t/2c$ relation at ϕ=90°; e is varied.

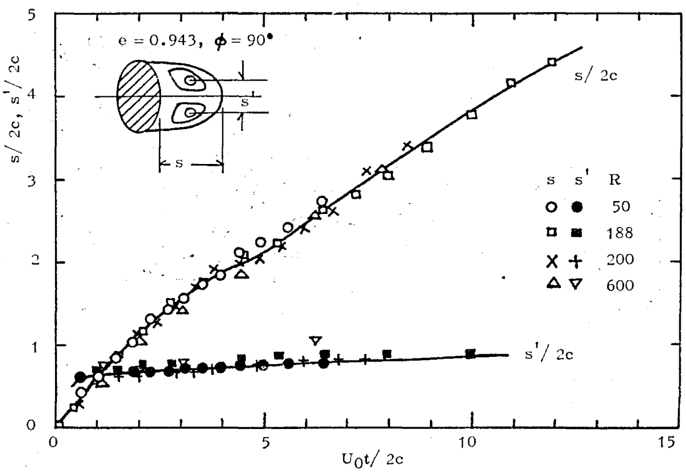

Fig. 10 $S/2c-U_0t/2c$ relation at ϕ=90°; R is varied.

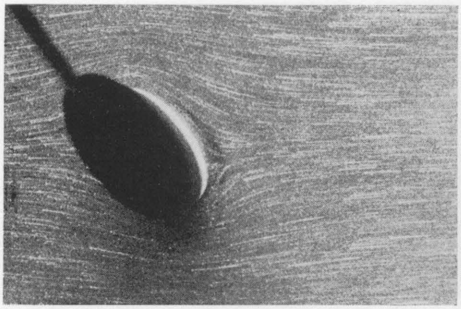

(a) $t = 0.750$ s, $U_0t/2c = 0.114$

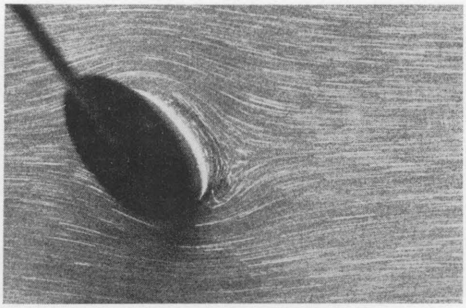

(b) $t = 4.00$ s, $U_0t/2c = 0.608$

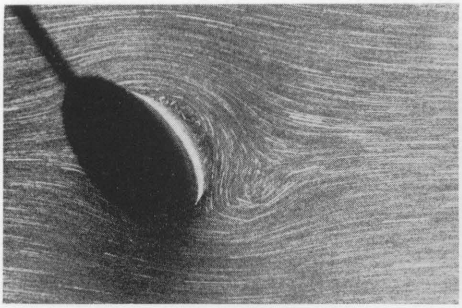

(c) $t = 7.25$ s, $U_0t/2c = 1.10$

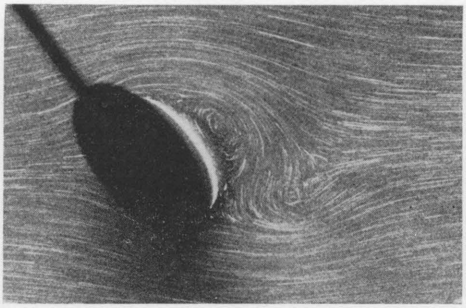

(d) $t = 10.7$ s, $U_0t/2c = 1.63$

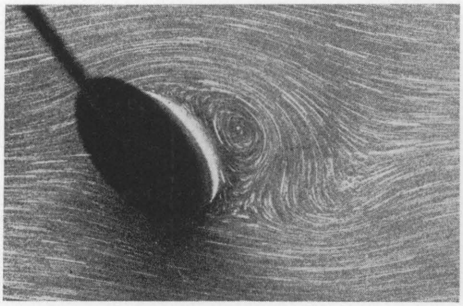

(e) $t = 14.0$ s, $U_0t/2c = 2.13$

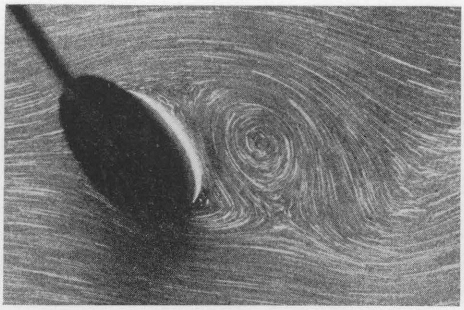

(f) $t = 20.4$ s, $U_0t/2c = 3.10$

Photo 3 Streamline sequence for an impulsively started elliptic cylinder at $R=164$; $U_0=0.552$ cm/s, $2c=3.64$, $e=0.866$, $\phi=54°$, $t_e=3.0$ s.

(*Facing* p. 278)

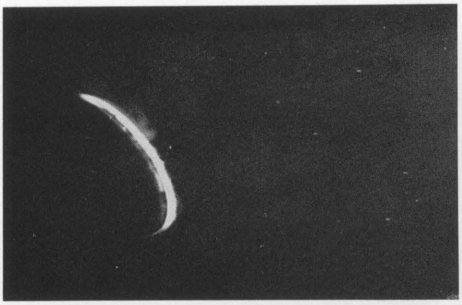

(a) $t = 2.50$ s, $U_0t/2c = 0.371$

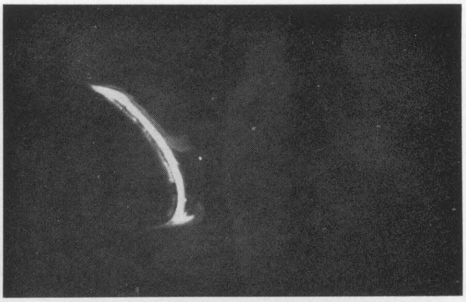

(b) $t = 5.00$ s. $U_0t/2c = 0.743$

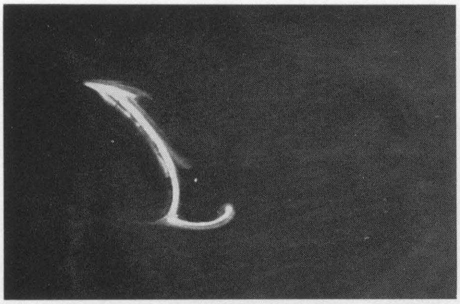

(c) $t = 8.50$ s, $U_0t/2c = 1.26$

(d) $t = 13.9$ s, $U_0t/2c = 2.06$

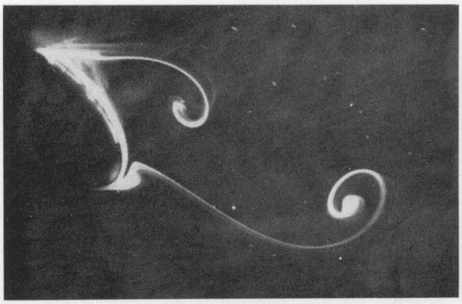

(e) $t = 21.8$ s, $U_0t/2c = 3.24$

(f) $t = 27.2$ s, $U_0t/2c = 4.04$

Photo 4 Separation of vortex sheets at $R=174$; $U_0 = 0.552$ cm/s, $2c=3.72$ cm, $e=0.865$, $\phi=54°$, $t_e=1/4$s.

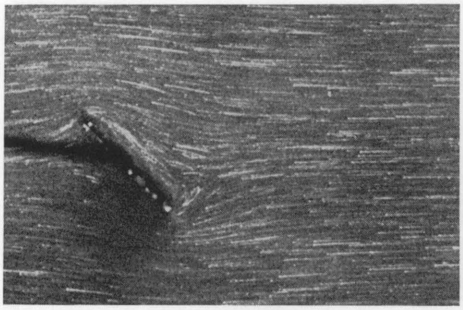

(a) $t = 0.950$ s, $U_0t/2c = 0.178$

(b) $t = 4.00$ s, $U_0t/2c = 0.750$

(c) $t = 7.60$ s, $U_0t/2c = 1.43$

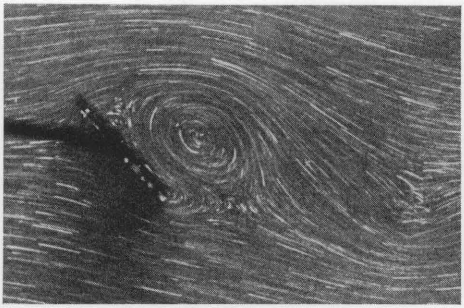

(d) $t = 13.6$ s, $U_0t/2c = 2.56$

(e) $t = 36.3$ s, $U_0t/2c = 6.82$

Photo 5 Streamline sequence for an impulsively started flat plate at $R=200$; $U_0=0.563$ cm/s, $2c=3.00$ cm, $\phi=45°$, $t_e=1.0$ s.

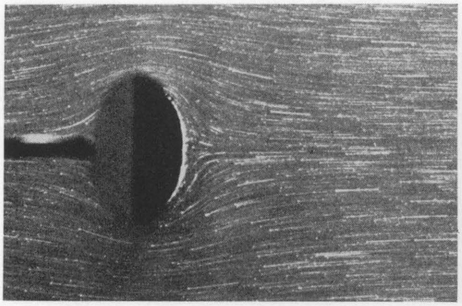

(a) $t = 0.600$ s, $U_0t/2c = 0.175$

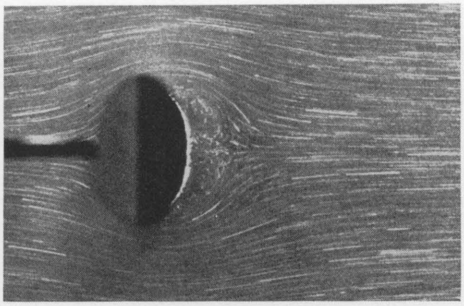

(b) $t = 3.10$ s, $U_0t/2c = 0.900$

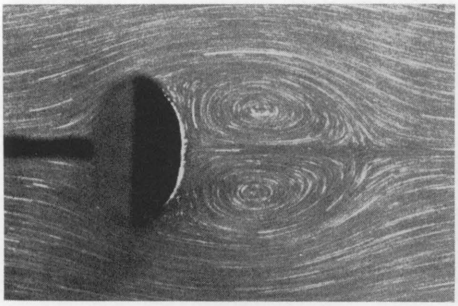

(c) $t = 14.4$ s, $U_0t/2c = 4.19$

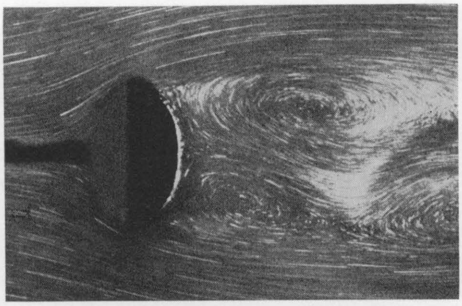

(d) $t = 57.8$ s, $U_0t/2c = 16.8$

Photo 6 Time dependent variation of flow pattern for an elliptic cylinder placed with its major axis normal to direction of uniform flow at $R = 200$; $U_0 = 0.707$ cm/s, $2c = 2.43$ cm, $e = 0.809$, $t_e = 2.0$ s.

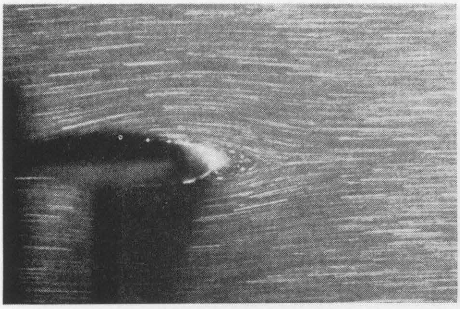

(a) $\phi=0°$, $t=6.90$ s, $U_0t/2c=1.49$, $U_0=0.610$ cm/s.

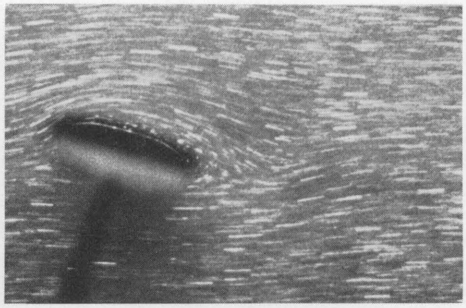

(b) $\phi=15°$, $t=6.10$ s, $U_0t/2c=1.38$, $U_0=0.640$ cm/s.

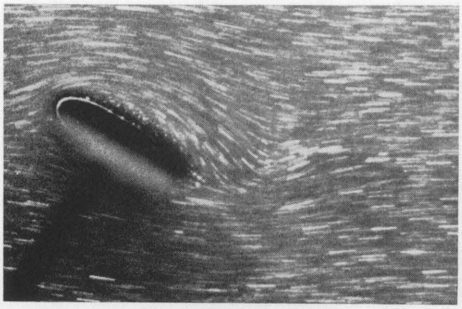

(c) $\phi=30°$, $t=6.60$ s, $U_0t/2c=1.48$, $U_0=0.636$ cm/s.

(d) $\phi=45°$, $t=7.00$ s, $U_0t/2c=1.60$, $U_0=0.650$ cm/s.

(e) $\phi=60°$, $t=6.20$ s, $U_0t/2c=1.38$, $U_0=0.629$ cm/s.

(f) $\phi=75°$, $t=6.15$ s, $U_0t/2c=1.36$, $U_0=0.629$ cm/s.

Photo 7 Comparison of flow patterns at various angles of attack when dimensionless time is 1.5 approximately; $R=200$, $e=0.943$.

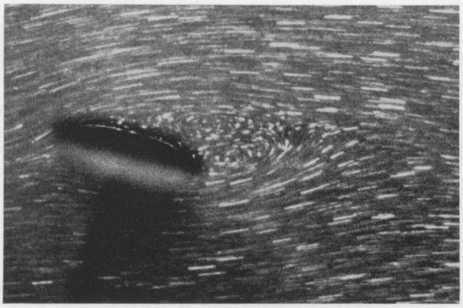

Photo 8 Twin vortices at a later stage of flow pattern evolution when ϕ is small; $R=200$, $e=0.943$, $\phi=15°$, $t=18.8$ s, $U_0t/2c=4.24$, $U_0=0.640$ cm/s.

leading edge of the body and the vortex center. There the agreement is good.

The flow pattern variation at $\phi=90°$ is displayed in Photo 6, which shows that symmetric twin vortices grow in a similar manner to the case of a circular cylinder. Fig. 9 shows the vortex length plotted against the time

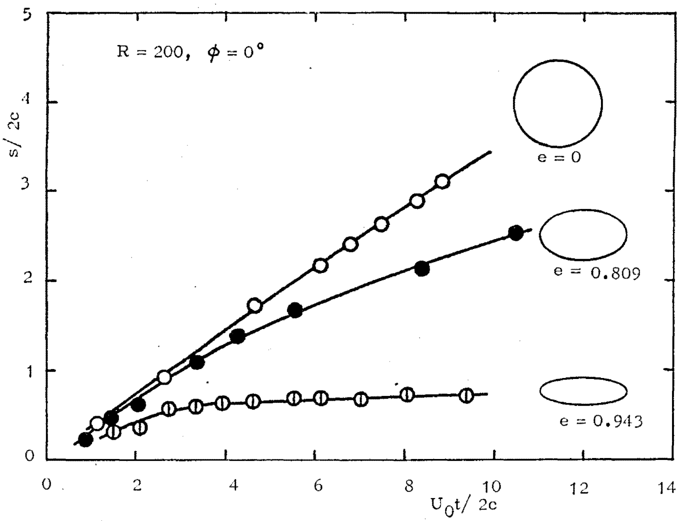

Fig. 11 $S/2c-U_0t/2c$ relation at $\phi=0°$; e is varied.

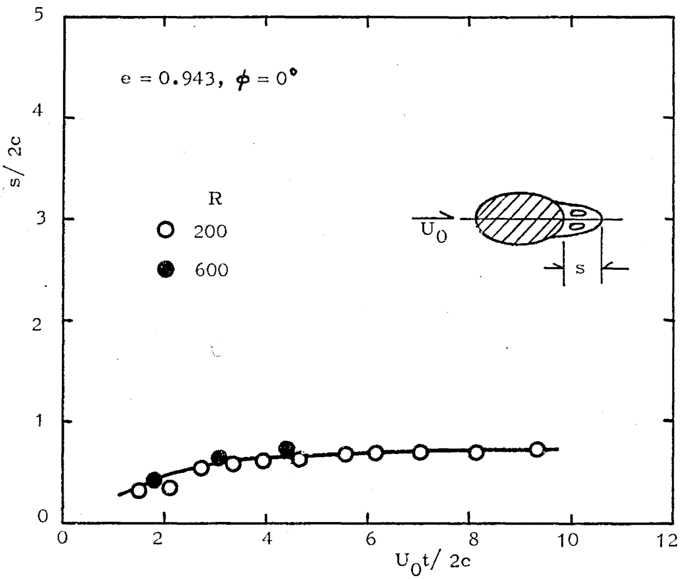

Fig. 12 $S/2c-U_0t/2c$ relation at $\phi=0°$; R is varied.

when e is varied. It should be noticed that the $s/2c-U_0t/2c$ curve seems to have a slight kink at $U_0t/2c \sim 4.5$. The physical reasoning for this slight anomaly is not yet evident. Fig. 10 shows the $s/2c-U_0t/2c$ relation at $\phi=90°$ when R is varied. The $s/2c-U_0t/2c$ relations at $\phi=0°$ are also shown in Figs. 11 and 12, when e and R are varied respectively. Tollmien[13] has pointed out that for an elliptic cylinder at $\phi=90°$ separation begins only at the rear stagnation point if $a^2/b^2<4/3$. In relation to this, it should be here noted that our a^2/b^2 are always larger than 4/3. In Photo 7 the flow pattern variation with ϕ is displayed at $R=200$ and $U_0t/2c=1.5$ approximately. As will be seen from the photographs, the closed wake bubble is large when ϕ is large, and especially at $\phi=75°$ the twin vortices are observed from early stages. When $U_0t/2c$ is large enough, however, twin but not symmetric vortices are observed even at $\phi=15°$, as shown in Photo 8.

5. Conclusion

Unsteady flow past spheres was investigated by means of a flow visualization technique. Similarly to the case of other types of unsteady flows, the irrotational flow is established at the beginning of motion. Then the symmetric vortex begins to grow. The time-wise variation of the ring vortex length was measured, and it was found that its time dependence is logarithmic. The critical time at which symmetry of the vortex is lost decreases with the increasing R. The embryo of the secondary vortex was observed upstream of the main vortex at $R=1500$.

Unsteady flow past elliptic cylinders was studied by means of the same method. It was observed that the irrotational flow pattern appears at the beginning of motion, and as time increases one wake bubble begins to develop on the downstream side of the test cylinder. The feature of the flow pattern variation agrees well with the calculated results of Lugt and Haussling. In the pattern variation no essential difference is found between the slender elliptic cylinder and the flat plate. The $s/2c-U_0t/2c$ curve has a slight kink at about $U_0t/2c=4.5$, and the pattern variation is affected considerably by the prescribed value of the angle of attack.

Acknowledgments

The author is grateful to Dr. H. J. Lugt for his helpful advice and for providing many figures of computed streamlines before publication. The author wishes to thank Professor S. Taneda for stimulating discussions and interest in this work, and Professor C. Y. Wang who called the author's attention to the problem treated here. The author also wish to acknowledge the help received from Miss S. Oka during later phases of this work.

References

1) Honji, H. and Taneda, S., Unsteady Flow past a Circular Cylinder, J. Phys. Soc. Japan, Vol. 27, 1969, p. 1668.
2) Honji, H. and Taneda, S., Time-Dependent Flow past a Circular Cylinder Accelerated from One Speed to Another, Rep. Res. Inst. Appl. Mech., Vol. 17, 1969, p. 187.
3) Taneda, S. and Honji, H., Unsteady Flow past a Flat Plate Normal to the Direction of Motion, J. Phys. Soc. Japan, Vol. 30, 1971, p. 269.
4) Rimon, Y. and Cheng, S. I., Numerical Solution of a Uniform Flow over a Sphere at Intermediate Reynolds Numbers, Phys. Fluids, Vol. 12, 1969, p. 949.
5) Boltze, E., Dissertation, 1908.
6) Wang, C. Y., Separation and Stall of an Impulsively Started Elliptic Cylinder, J. Appl. Mech., 1967, p. 823.
7) Lugt, H. J. and Haussling, H. J., Laminar Flows past a Flat Plate at Various Angles of Attack, Presented at the 2 nd Int'l Conf. on Numerical Methods in Fluid Dynamics, Univ. of California, Berkeley, Sept. 15-19, 1970. Also, Lugt, H. J. and Haussling, H. J., Laminar Flows Past Elliptic Cylinders at Various Angles of Attack, Naval Ship Research and Development Center Report No. 3748, 1972.
8) Fage, A. and Johansen, F. C., On the Flow of Air behind an Inclined Flat Plate of Infinite Span, Proc. Roy. Soc. London, A Vol. 116, 1927, p. 170.
9) Richards, G. J., On the Motion of an Elliptic Cylinder Through a Viscous Fluid, Phil. Trans., A Vol. 233, 1934, p. 279.
10) Taneda, S., Studies on Wake Vortices (III)-Experimental Investigation of the Wake behind a Sphere at Low Reynolds Numbers, Rep. Res. Inst. Appl. Mech., Vol. 4, 1956, p. 99.
11) Hamielec, A. E. and Raal, J. D., Numerical Studies of Viscous Flow around Circular Cylinders, Phys. Fluids, Vol. 12, 1969, p. 11.
12) Kochin, N. E., Kibel, I. A., and Rose, N. V., *Theoretical Hydromechanics*, 1965, Interscience.
13) Tollmien, W., Grenzschichten, *Handb. Exper. Physik*, Vol. 4, 1931, p. 241.

(Received Nov. 17, 1971)